the reactivity of the rocks, the geologic contact time, and the degree of weathering (including oxidation) of the fracture surfaces through which migration occurs (*14*). In establishing geologic storage as an acceptable means of isolating long-lived radionuclides from people, it is important that all the factors that control solution concentrations be taken into consideration in assessing the risks.

E. A. BONDIETTI
C. W. FRANCIS
Environmental Sciences Division, Oak Ridge National Laboratory, Oak Ridge, Tennessee 37830

References and Notes

1. "Alternatives for managing wastes from reactors and post-fission operations in the LWR fuel cycles" (Publication 76-43, Energy Research and Development Administration, Washington, D.C., 1976), vol. 4.
2. R. C. Rouston, G. Jansen, A. V. Robinson, "Sorption of Tc-99, Np-237, and Am-241 on two subsoils from differing weathering intensity areas" (Report BNWL-1889, Battelle Pacific Northwest Laboratories, Richland, Wash., March 1973); B. Allard, H. Kipatsi, J. Rydberg, "The sorption of long-lived fission products and actinides on natural clay and rock minerals" (preliminary report of Project KBS 19:01 for the period 15 February to 15 June 1977, Department of Nuclear Chemistry, Chalmers University of Technology, Göteborg, Sweden).
3. G. de Marsily, E. Ledoux, A. Barbreau, J. Margat, *Science* **197**, 519 (1977).
4. R. M. Garrels and C. L. Christ, *Solutions, Minerals, and Equilibria* (Harper & Row, New York, 1965).
5. M. Pourbaix, *Atlas of Electrochemical Equilibria* (Pergamon, New York, 1966). The equations used for calculating the lines in Fig. 1a are as follows: for TcO_4^-/TcO_2, $E_0 = 0.738 - 0.0788\ pH + 0.0197 \log (TcO_4^-)$; for NpO_2^+/NpO_2, $E_0 = 0.564 + 0.0591 \log (NpO_2^+)$ (E_0 is the equilibrium potential). Selection of $Np(OH)_4$ would substitute 0.534 V.
6. Waste Isolation Safety Assessment Program (WISAP), managed by Battelle Pacific Northwest Laboratories, Richland, Wash. The rock samples were provided by R. J. Serne. The three igneous rocks were Sentinel Gap basalt (Mattawa, Wash.), Westerly granite (New Hampshire), and Climax Stock granite (Nevada). The three shales consisted of green argillaceous shale (New York, Wards Scientific Establishment 47W-7400) and Conasauga shales (surface and subsurface). These rocks and shales were crushed to ≤ 50 mesh with a ceramic mortar and pestle. The isotopes ^{99}Tc, ^{237}Np, and ^{239}Np were obtained from the Oak Ridge National Laboratory; ^{95m}Tc was obtained from Argonne National Laboratory, Argonne, Ill. The ^{95m}Tc was isotopically pure, having been made by the $^{93}Nb(\alpha, 2n)^{95m}Tc$ reaction.
7. After the *p*H of the rock-water slurries had been established, the cell was supplemented with a miniature Pt electrode (0.03 cm^2) in place of the glass electrode (there were now two Pt electrodes in the cell). The Pt electrode with the larger surface area consistently measured more negative potentials than the Pt electrode with the smaller surface area, although there was never more than a 40-mV difference. The *Eh* values recorded in Fig. 1a were based on measurements from the larger electrode. There is no certainty that the Pt electrode is really responsive to the true Fe^{2+}/Fe^{3+} activity in solution since the concentrations would be very low. Oxygen could also be limiting the attainment of potentials lower than observed.
8. International Commission on Radiological Protection (ICRP), "Report of Committee II on permissible dose for internal radiation (1959)," *Health Phys.* **3**, 1 (June 1960). The ICRP recommendation that the maximum permissible concentrations for the general public be 1/10 of the occupational limit was followed for the calculations. Concentrations used were $^{99}TcO_4^-$, 0.11 μM, and $^{237}NpO_2^+$, 16 nM.
9. The basalt particles were packed into a glass column 23 by 1.5 cm. A dual-tagged (^3H and Tc) simulated basalt groundwater (*p*H 8.10) was made up containing the following ions (in milligrams per liter): Na^+, 30; K^+, 9; Ca^{2+}, 6.5; Mg^{2+}, 1.0; HCO_3^-, 58; SO_4^{2-}, 23; Cl^-, 16; and F^-, 0.7. This solution was slowly added to the column under anoxic conditions (9 ml to 57 g of 18- to 35-mesh basalt). Nontritiated water was used to displace portions of the surface-associated groundwater. The Tc recovery was referenced to the ^3H concentration.
10. The Np(IV) was distinguished from Np(V) by zirconium phenylarsonate precipitation [A. F. Voigt, N. R. Sleight, R. E. Hein, J. M. Wright, in *The Transuranium Elements*, G. T. Seaborg, J. J. Katz, W. M. Manning, Eds. (McGraw-Hill, New York, 1949) (part II), pp. 1119–1127]. Citric acid (0.1M) was used to extract Np from the igneous rocks, and 1M $(NH_4)_2CO_3$ was used for the Conasauga shale [citric acid extracted significant amounts of Fe(II), which reduced Np(V) during the precipitation procedure]. The carbonate extract was acidified to 0.5M HCl before precipitating zirconium phenylarsonate. Extractions of Np from the rocks were conducted for 1 minute. The precipitation procedure often results in some precipitation of Np even if Np(V) is the only oxidation state present. Thus a 1 to 3 percent Np(IV) value may not be significant evidence for the presence of Np(IV). Values greater than this are stronger evidence for the presence of Np(IV).
11. E. A. Bondietti and F. H. Sweeton, in *Proceedings, Symposium on Transuranium Elements in Natural Environments*, M. G. White and P. B. Dunaway, Eds. (Publication NVO-178, Energy Research and Development Administration, Washington, D.C., 1977), pp. 449-476.
12. V. S. Dement'yev and N. G. Syromyatnikov, *Geochemistry (USSR)* **2**, 141 (1965).
13. C. F. Baes and R. E. Mesmer, *The Hydrolysis of Cations* (Wiley-Interscience, New York, 1976).
14. Recent Swedish experiments on the in situ migration of ^{99m}Tc in fractured granite (80-m depth and residence times of several days) have not indicated the reduction of Tc (B. G. F. Carleson, AB Atomenergi Studsvik, Nykoping, Sweden, personal communication). However, it is anticipated that the Swedish radioactive waste repository will be located at 500 to 800 m in less weathered granite.
15. We thank J. N. Brantley and F. S. Brinkley for technical assistance and T. E. Cerling and S. Y. Lee for reading the manuscript and offering helpful suggestions. Research supported by the Office of Health and Environmental Research and the Waste Isolation Safety Assessment Program, U.S. Department of Energy, under contract W-7405-eng-26 with Union Carbide Corporation. Environmental Sciences Division Publication No. 1330.

13 April 1978; revised 26 December 1978

Variable Porosity in Siliceous Skeletons: Determination and Importance

Abstract. *Gas adsorption data were used to obtain the specific surface area and specific pore volume for a variety of biogenically precipitated silica samples. The results suggest that this material is finely divided and porous. This interpretation was corroborated by the use of transmission electron microscopy at magnifications up to 180,000.*

Box model calculations involving the geochemical cycle of silica in the oceans (*1*) suggest that at least ten times as much silica is annually precipitated by single-celled plants and animals (*2*) as is delivered to the oceans by rivers or preserved in sediments. Although the order in which a few species of organisms disappear with time or with depth in the water column has been observed in laboratory (*3*) and field (*4*) studies, the mechanism by which one species is better preserved than another under the same set of conditions is still poorly understood. In this report we present techniques for studying the porous ultrastructure of biogenically precipitated silica. Study of this structure will help to elucidate (i) mechanisms behind skeleton precipitation, (ii) recycling rates of silica in the water column, (iii) resistance of the skeleton to breakage during predation, (iv) settling rates of skeletons through the water column, (v) preservation of skeletons in the water column and sediments, and (vi) quantitative morphological and diagenetic structural changes in the skeletons.

We have begun to characterize the physical and chemical properties of the siliceous frustules, spicules, and skeletons of diatoms, sponges, and radiolarians. We studied changes with age in specific surface area, solubility, and dissolution rate (*5*) and density, refractive index, and water content (*6*). We now describe a methodology for the quantification of skeletal porosity and specific pore volume and discuss the importance of the relationship of specific pore volume to specific surface area.

Sample cleaning methods and the specific surface area measurement technique have been described elsewhere (*5*, *7*). A similar approach was used to estimate specific pore volumes (*8*) for each of the samples studied. It is important to note that surface area and pore volume measurements must be made on the same sample. Within one assemblage we have measured specific surface areas that differed from one another by a factor of 3 or more, depending on the species composition of one sample relative to the next. The data presented here are averages for well-mixed assemblages.

Sample ages range from present day to 40 million years ago and contain mostly radiolarians with lesser amounts of diatoms and sponge spicules. The overall dimensions of radiolarians vary from about 50 to 500 μm and the specific surface areas measured vary from about 2 to 130×10^4 cm^2/g, suggesting that the

0036-8075/79/0330-1340$00.50/0

structural elements of their skeletons may be composed of a network of finely divided material (*5, 9, 10*).

It is possible to estimate the approximate spacing of these finely divided particles from the equation

$$r = \frac{2V}{\gamma A} \quad (1)$$

where V is the specific pore volume (cm^3/g), A is the specific surface in (cm^2/g), r is the mean pore radius or half the distance between adjacent surfaces, and γ is a shape factor based on the geometry of the system (*11-13*). Figure 1 is a plot of pore volume against surface area (*9*). It is evident from Fig. 1 that (i) the actual value of r is small—in the range 25 to 45 Å—and of the same approximate order as the low estimates of particle sizes based on specific surface area measurements (*11*); and (ii) the range of r is relatively small, suggesting either that different assemblages have similar values of r or that most of the assemblages studied have similar distributions of r values. If the ranges or distributions of ranges of interparticle spacings are similar, then the mechanisms for precipitation of silica on an ultrastructural level during the time interval studied may have been similar because this measure of ultrastructural morphology does not seem to have changed greatly.

But if the value of r or its distribution is more or less unchanging, why do surface areas and pore volumes vary by nearly two orders of magnitude? Everett (*13*) suggested that if a solid consists of a mixture of two components, one uniformly porous and the other essentially nonporous (*14*), then by varying the ratio of these components, we can vary both specific pore volume and specific surface area but maintain a fairly constant value of r (*15*). Thus if, on the average, the skeletons of the radiolarians in one assemblage consisted primarily of the nonporous end-member and those in a different assemblage consisted predominantly of the porous end-member, the latter would have somewhat higher values of pore volume and area but could still have the same value of r.

The position of one assemblage relative to another in Fig. 1 should suggest whether, under equivalent sets of environmental conditions, that assemblage would be likely to be better or more poorly preserved. We think this is so because our models for silica dissolution (*5, 10*) are based on specific surface area measurements which allow us to estimate a mean particle size for a particular assemblage. Given the mean particle size, it is possible to estimate the lifetime of this particle as a function of temperature and the degree of decomposition of its original surrounding protoplasm. The more porous an assemblage or an individual species is, the smaller is its mean particle size (*16*) and the more rapidly will it both dissolve and mechanically break up.

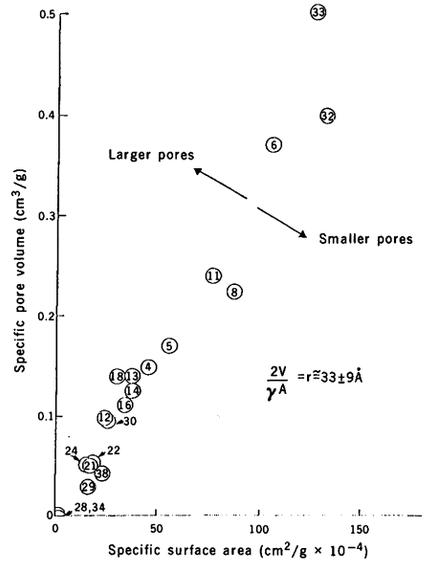

Fig. 1. Specific pore volume versus specific surface area for a variety of acid-cleaned, predominantly radiolarian assemblages. Gamma is a shape factor (*13*) with a suggested value of 2, and r is the mean pore radius or interparticle half-spacing. Note that the value of r is small and that its range is narrow.

To test the validity of Everett's porous-nonporous model as applied to our data, and to determine which of Everett's structural geometric models most closely approximates biogenically precipitated silica, we used transmission electron microscopy to examine many of the radiolarian and diatom species used for Johnson's dissolution index (*4*), as well as a few Miocene and Eocene samples (*17*). Figure 2 shows sections through one of the structural elements of a Recent radiolarian, *Theocalyptra* sp. (Fig. 2a), several frustules of a Recent diatom, *Ethmodiscus rex* (Fig. 2b), a frustule of a Recent diatom, *Coscinodiscus* sp. (Fig. 2c), and a Miocene radiolarian skeletal member, *Spongaster* sp. (Fig. 2d). The parallel, conchoidal fractures of the central core (~1300 to 1500 Å in width) are artifacts of the sectioning process and are not inherent in the organisms' structures. The darker portions of the skeleton represent electron-dense material, and the lighter areas have less of the same substance.

Everett's model does not require that the nonporous material be in the center of the frustule, but only that the proportions of porous to nonporous vary. In all the species we studied thus far, however, a central core of relatively nonporous silica is surrounded by a layer of considerably more porous material. The volume percentages of the two layers vary as a function of species and may be affected by the development of the skeleton during the lifetime of the organism and the skeleton's alteration with time after its death. Relatively low-resolution transmission electron microscopy studies of diatom (*18*), silicoflagellate (*19*), and sponge (*20*) silica and sponge cal-

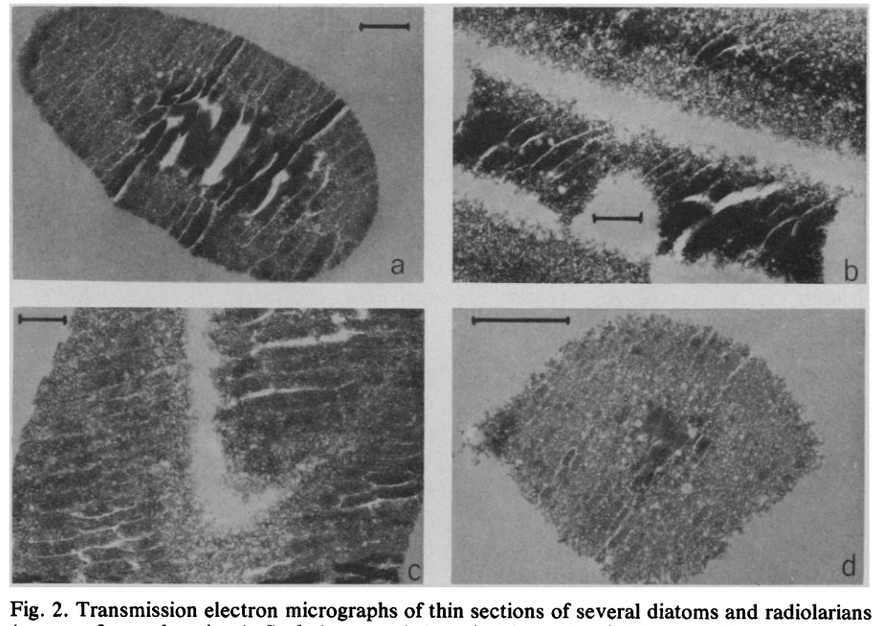

Fig. 2. Transmission electron micrographs of thin sections of several diatoms and radiolarians (see text for explanations). Scale bars are 0.5 μm in (a) to (c) and 1.0 μm in (d).

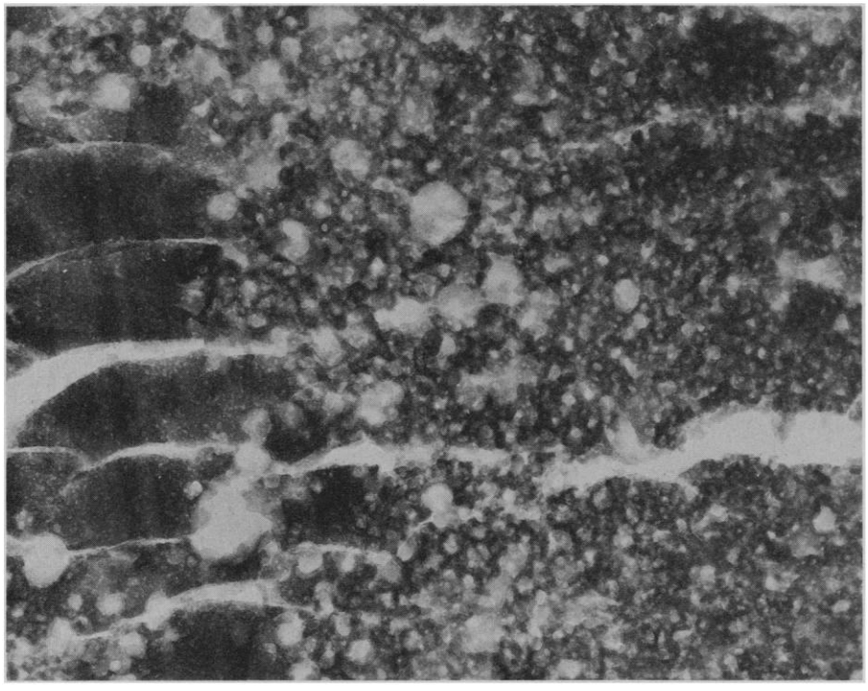

Fig. 3. Higher-resolution micrograph (×90,000; 1 mm = 150 Å) of a portion of the Miocene *Spongaster* sp. skeleton section in Fig. 2d. Note the large number of open pores in the outer structure and what appear to be closed pores in the less porous core structure.

cium carbonate (*21*) precipitation in organisms have suggested similar gross morphology, but skeletal porosities, particle sizes, and surface areas were not determined quantitatively.

Figure 3 shows additional details of the solid structural geometry of a portion of Fig. 2d. Close inspection reveals an extremely large number of pores, many of which are within the range of our size estimates in Fig. 1. The three-dimensional structure of the porous layer is complex and is not exactly like any of Everett's models, although an interconnected rod model with a statistical distribution of rod thicknesses and spacings would probably be closest. What we have referred to as the nonporous layer does, in fact, have pores, although many of these may be closed.

Both specific surface area and specific pore volume generally decrease with increasing sample age (*9*). Moore (*22*) showed that radiolarian test weights increase by a factor of about 3 during the time period Recent to 40 million years before present. The pore volumes of our samples decrease by a factor of about 50 (Fig. 1), although the range of r values remains essentially unchanged. If the gross dimensions of the tests remained about the same during this time period, then infilling of all the pores of Recent radiolarians would increase their skeletal bulk density from about 1.7 to 2.1 g/cm^3 (*23*). For test weights to increase by a factor of about 3 would require either infilling of the pores of older radiolarians with a denser polymorph of silica (cristobalite, tridymite, or quartz) or skeletal volumes of Eocene radiolarians that were about 2^1/$_2$ times greater than those of Recent ones, or some combination of these factors. We do not have enough data at this time to unambiguously choose between these interpretations or determine their relative importance.

In conclusion, we suggest that the siliceous skeletons of radiolarians—and perhaps diatoms and sponges as well—are porous to varying degrees. The porosity and mean pore size can be quantified by gas adsorption data and observed with transmission electron microscopy.

DAVID C. HURD
Department of Oceanography and Hawaii Institute of Geophysics, University of Hawaii, Honolulu 96822

CHIYE WENKAM
Scripps Institution of Oceanography, Geological Research Division, University of California at San Diego, La Jolla 92037

H. STUART PANKRATZ
Department of Microbiology and Public Health, Michigan State University, East Lansing 48824

JAMES FUGATE
U.S. Geological Survey, Corpus Christi, Texas 78411

References and Notes

1. W. Broecker, *Chemical Oceanography* (Harcourt Brace Jovanovich, New York, 1974), pp. 3–29; R. M. Garrels and F. T. Mackenzie, *Evolution of Sedimentary Rocks* (Norton, New York, 1971), pp. 95–115.
2. Organisms predominantly responsible for silica precipitation in near-surface waters are diatoms, radiolarians, and silicoflagellates.
3. T. Johnson, *Deep-Sea Res.* **21**, 851 (1974).
4. O. G. Kozlova, *Diatoms of the Indian and Pacific Sectors of the Antarctic* (Israel Program for Scientific Translations, Jerusalem, 1966); H. J. Schrader, in *First Symposium on Recent and Fossil Marine Diatoms*, R. Simonsen, Ed. (Cramer, Bremerhaven, 1972), pp. 191–216; M. Ohwada, *Mem. Kobe Mar. Obs. Kobe Jpn.* **14**, 1 (1960).
5. D. C. Hurd and F. Theyer, in *Analytical Methods in Oceanography*, T. R. P. Gibb, Jr., Ed. (American Chemical Society, Washington, D.C., 1975), p. 211.
6. ———, *Am. J. Sci.* **277**, 1168 (1977).
7. Briefly, samples are separated from sediment with a 60-μm mesh sieve and treated for several hours to days at 60° to 80°C with dilute HCl and ultrasonics until a microscopically clean appearance is achieved. Sample assemblage surface areas are then estimated by using a three-point BET calculation [Gregg and Sing (*8*)] with nitrogen as the adsorbing gas.
8. S. J. Gregg and K. S. W. Sing [*Adsorption, Surface Area and Porosity* (Academic Press, London, 1967), chaps. 2 and 3] gave general approaches for determining specific pore volumes by using a variety of adsorbates and partial pressures. We first filled all the pores of the sample by flowing pure nitrogen gas over it and then switched to a mixture of 98 percent nitrogen and 2 percent helium. Depending on pore geometry, this approach yields the volume of all pores less than 250 to 500 Å in radius. These experiments could be duplicated in a vacuum desiccator at room temperature by using CCl_4 or water vapor at 98 percent saturation and measuring sample weight changes; note that the sample must be preheated in a vacuum oven at 150°C for several hours to remove molecular water adsorbed earlier from the air.
9. The following sample ages, in million years (MY) before present, correspond to the sample numbers: Recent, 32 and 33; 2 MY, 4, 5, and 6; 4.6 MY, 8; 6.4 MY, 11 and 12; 8 MY, 13 and 14; 10 MY, 16; 13 to 15 MY, 18 and 21; 18 MY, 38 and 22; 21 MY, 24; 34 to 38 MY, 29 and 30; and 40 MY, 28 and 34. All surface areas were redetermined for this study.
10. D. Lawson, D. C. Hurd, H. S. Pankratz, *Am. J. Sci.* **278**, 1373 (1978).
11. For example, if the solid were composed of a collection of small spheres having a density of 2.2 g/cm^3, then the surface areas would correspond to sphere diameters of 0.021 to 1.35 μm; interconnected rods would yield smaller diameters.
12. Gregg and Sing (*8*) give the derivation of Eq. 1 in chapter 3.
13. D. H. Everett [in *The Structure and Properties of Porous Materials*, D. H. Everett and F. S. Stone, Eds. (Butterworth, London, 1958), p. 95] gives a more extensive treatment involving a variety of solid geometries. Note that γ is liquid surface tension in Gregg and Sing (*8*) but is a shape factor in Everett.
14. The nonporous end-member for Fig. 1 might have a specific surface area value equivalent to the thickness of the main structural element of the skeleton. The porous portion might have, if not uniform, at least constant overall porosity, and values for this end-member of 0.6 to 0.7 cm^3/g and 200 × 10^4 cm^2/g are reasonable.
15. The constancy of the value of r depends on the structural geometry of the system, as Everett (*13*) shows in his figure 8; in general, ratios of pore volume to surface area are linear.
16. The lower limit of particle size will depend on the properties of the porous end-member.
17. Samples of acid-cleaned material were embedded in methylene blue–stained noble agar, dehydrated with a series of alcohol dilutions, washed with propylene oxide, and the agar chip embedded in Spurr resin. Using a diamond knife, the samples were cut into sections ~ 500 Å thick, placed on a 300 mesh grid, and photographed with a Phillips 300 transmission electron microscope at 80 to 100 keV.
18. P. A. Dawson, *J. Phycol.* **9**, 353 (1973); R. W. Drum and H. S. Pankratz, *J. Ultrastruct. Res.* **10**, 217 (1964); B. E. F. Reimann, J. C. Lewin, B. E. F. Volcani, *J. Phycol.* **2**, 74 (1966); E. F. Stoermer, H. S. Pankratz, C. C. Bowen, *Am. J. Bot.* **52**, 1067 (1965).
19. S. D. Van Valkenburg, *J. Phycol.* **7**, 113 (1971).

20. T. L. Simpson and C. A. Vaccaro, *J. Ultrastruct. Res.* **47**, 296 (1974).
21. D. G. Dunkelberger and N. Watanabe, *Tissue Cell* **6**, 573 (1974).
22. T. C. Moore, *Geol. Soc. Am. Bull.* **80**, 2103 (1969).
23. Extrapolation of a plot of the pore volume data in Fig. 1 against skeletal density as obtained from "heavy" liquid separation techniques (5) yields a value of about 2.1 g/cm³ at zero pore volume. It is possible that failure to obtain higher density values was partly due to the existence of closed pores in the nonporous core of the skeletons.
24. We thank S. V. Smith, H. Schrader, H. Sachs, L. Small, and R. Young for critical comments on various drafts of this report. We also thank H. Morrow, E. Porta, and R. Allen for the use of their supplies and facilities. Supported by ONR and by NSF grants OCE 77-20446 and OCE 78-08697. This is Hawaii Institute of Geophysics Contribution 933.

18 September 1978; revised 14 December 1978

Distribution of Transmembrane Polypeptides in Freeze Fracture

Abstract. *Human erythrocytes have been freeze-fractured, and the polypeptides associated with the separate halves of the membrane bilayer have been analyzed by sodium dodecyl sulfate polyacrylamide gel electrophoresis. The transmembrane proteins were differentially separated by the fracture process. Although sialoglycoproteins associated with the outer half of the membrane, the anion transport protein (band 3) mainly remained with the inner half of the membrane. Well-defined fragments of the sialoglycoproteins were produced by the freeze-fracture procedure, indicating that selected covalent bonds of these transmembrane proteins were broken.*

The lipid bilayer of biological membranes is readily split during freeze fracture (*1*). Until recently, however, there has been no technique for differentially analyzing the two halves of a membrane biochemically. This difficult task of physically isolating sufficient quantities of half-membranes has recently been overcome by freezing a monolayer of erythrocytes between a polylysine-coated cover slip and a copper plate (*2*). When this sandwich is fractured at liquid nitrogen temperature by separating the glass from the copper, the portion of the membrane's external lipid layer that is in direct contact with the polylysine-coated cover slip remains associated with the cover slip, while the remainder of the structure, including the inside half of the fractured membrane, remains with the copper plate (*2*).

The distribution of membrane proteins in the freeze-fracture process has not been satisfactorily explained. The "bumps" produced in the process have been assumed to be the transmembrane proteins (*3*, *4*) that extend through the lipid bilayer, and the disposition of the bumps with respect to each other is taken to reflect the organization of proteins within the plane of the membrane. We investigated the distribution of membrane polypeptides associated with the two halves of the membrane bilayer, employing the technique of Fisher (*2*). Since most, if not all, of the major proteins exposed on the outside surface of the human erythrocyte membrane have been shown to be transmembrane (*5*), the erythrocyte is an especially good membrane for this study of the organization of plasma membrane proteins.

Preparations of cells, cover slips, and copper plates were similar to those used by Fisher (*2*). Number 1 cover slips measuring 24 by 50 mm were soaked overnight in chromic acid, rinsed with distilled water, dried with nitrogen, covered on one side with 0.1 ml of 5 m*M* polylysine (molecular weight, 3400; Sigma), rinsed with distilled water, and again dried with nitrogen. A flat, cold-rolled copper sheet 0.51 mm thick was cut into 76 by 32 mm plates. Nonflat plates were culled, and the rest were polished and then etched with a 1 : 1 mixture of concentrated nitric acid and water for 15 seconds, rinsed five times in distilled water, and then nitrogen-dried. The cover slips and copper plates were prepared no more than 1 day before the experiment and were kept in a covered container until used.

Erythrocytes from freshly drawn human blood (acid citrate dextrose anticoagulant) were washed three times in isotonic saline and then once in isotonic phosphate buffer, *p*H 7.4. Cells were radioactively labeled by either lactoperoxidase-catalyzed ^{125}I iodination (*5*) or periodate treatment followed by reduction with tritiated sodium borohydride (*6*, *7*). After rinsing and centrifuging several times in phosphate-buffered saline (PBS) to remove unincorporated label, the cells were centrifuged for 10 minutes at 1000*g* in a graduated test tube, decanted, and resuspended in a volume of PBS equal to 0.4 of their own volume. This results in a cell density of 6×10^9 to 7×10^9 erythrocytes per milliliter.

This cell suspension (0.2 ml) was distributed over the surface of the polylysine-coated cover slip. Cells not bound

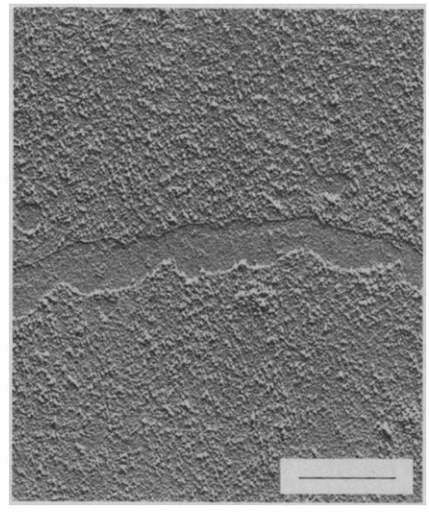

Fig. 1 (left). Replica of the E faces of freeze-fractured human erythrocytes that had been bound to a polylysine-coated cover slip. Shown are portions from two cells with the intervening gap. The marker is 0.5 μm long.

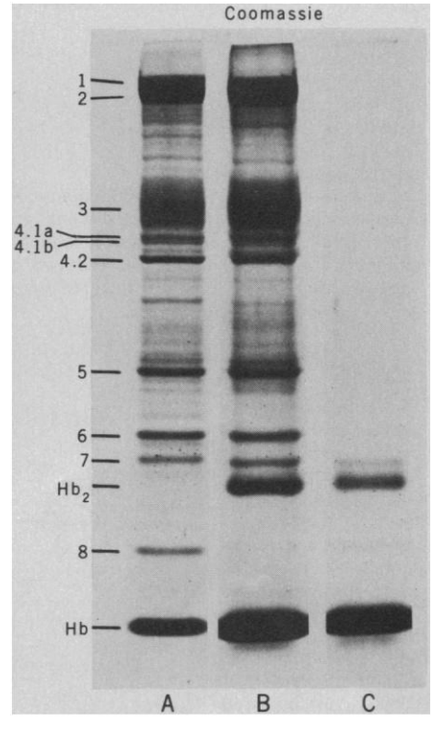

Fig. 2 (right). Coomassie blue profile of erythrocyte membrane polypeptides separated by electrophoresis on 7.5 to 15 percent linear acrylamide gradient gels, using the SDS discontinuous buffer system of Laemmli (*6*, *22*). Lane *A* contains polypeptides from the unfractured membranes of $120 \pm 10 \times 10^6$ erythrocytes. The membrane proteins recovered from the freeze-fracture sample are shown in lane *B* (fractured cells from the copper plate plus an undetermined number of unfractured cells) and lane *C* (cover slip sample, equivalent to the complete E faces of $40 \pm 10 \times 10^6$ cells). The latter value assumes 20×10^6 fracture cells per cover slip with an average of one-third of each cell's membrane being fractured (*2*). Stroma proteins were numbered according to Fairbanks *et al.* (*12*). Abbreviations: *Hb*, hemoblogin; Hb_2, apparent hemoglobin dimer.

0036-8075/79/0330-1343$00.50/0